ELSEVIER

Journal of Alloys and Compounds 279 (1998) 279–286

Journal of ALLOYS AND COMPOUNDS

Thermal stability and hydriding properties of nanocrystalline melt-spun $Mg_{63}Ni_{30}Y_7$ alloy

Tony Spassov[1,*], Uwe Köster

Dept. Chem. Eng., University of Dortmund, D-44221 Dortmund, Germany

Received 22 May 1998

Abstract

Nanocrystalline $Mg_2(Ni,Y)$ hydrogen storage alloy (with exact composition $Mg_{63}Ni_{30}Y_7$) was prepared by rapid solidification, using a melt-spinning technique. Thermal stability and phase transition in the as-quenched alloy were studied by TEM, DSC, X-ray and electron diffraction. It was found that the as-cast material consists of mainly hexagonal $Mg_2(Ni,Y)$ nanocrystals with an average size of 2–3 nm and a significant amount of amorphous phase with similar composition located between them. During heating the alloy crystallizes completely by three dimensional nanocrystal growth, with an activation energy of 140 ± 7 kJ mol^{-1}. The hydriding properties of the as-quenched nanocrystalline alloy were studied as well. The maximum hydrogen absorption capacity (about 3.0 wt.%) and hydrogenation kinetics of the melt-spun $Mg_2(Ni,Y)$ were found to exceed those of the conventionally prepared polycrystalline Mg_2Ni alloys and to be comparable to the hydrogen absorption characteristics of nanocrystalline ball-milled Mg_2Ni. Hydrogenation of the as-cast alloy causes a change in the crystallization mechanism during annealing, as the microstructure remains nanocrystalline (15–20 nm) even after complete crystallization of the alloy.

Keywords: Magnesium alloys; Rapid quenching; Nanocrystalline; Amorphous alloy; Hydrogen storage

1. Introduction

Magnesium and magnesium–nickel alloys have been intensively studied during the last decades as potential candidates for hydrogen storage systems. Due to their higher hydrogen capacity, lower specific weight and richer natural resources, as compared with other hydrogen storage alloys, they are considered as the most promising alloys for storing hydrogen. Among all Mg-based alloys intermetallic Mg_2Ni is an alloy of largest interest for H-storage, because of its relatively high hydrogen capacity (up to 3.6 wt.% [1]) and higher stability in air compared with pure Mg and some other H-storage systems. Another disadvantage of pure Mg is its high hydrogen desorption temperature (about 300°C) and very low kinetics, which places it far from practical application. Mg_2Ni–H is also one of the most suitable hydride systems for heat storage, because of the large enthalpy of hydride formation and high capacity of hydrogen storage [2].

Nanocrystalline hydrides (incl. nanocrystalline Mg_2Ni-based alloys) are a new class of H-storage systems, which combine good H-absorption capacity, increased rates of hydriding/dehydriding, enhanced mechanical properties and microstructural stability. The high surface to volume ratios (high specific surface area) and the presence of large number of grain boundaries in nanocrystalline alloys enhance the kinetics of hydrogen absorption/desorption. On the other hand, by reducing the particle size the decrepitation of the particles upon repeated hydrogenation can be avoided [3].

Zaluski et al. [4,5] as well as Orimo et al. [6,7] showed that the hydriding/dehydriding properties at low temperatures (lower than 200°C) of nanocrystalline Mg_2Ni alloys, prepared by mechanical alloying (by high energy ball-milling), can be improved by reducing the grain size (20–30 nm), due to hydrogen occupation in the disordered interface phase. Not so much attention, however, has been devoted to investigating the hydriding characteristics of nanocrystalline Mg–Ni alloys, produced by rapid solidification (e.g. melt-spinning) or by crystallization of amorphous precursors. It is known, that by rapid quenching from the melt, different metastable materials (as amorphous, nanocrystalline, quasicrystalline, polycrystalline) can be produced, as well as desirable crystal sizes and

*Corresponding author.

[1]On leave from: Dept. Chem., University of Sofia, 1126-Sofia, Bulgaria.

0925-8388/98/$ – see front matter
PII: S0925-8388(98)00680-X

morphology can be attained. Besides, metallic glasses can serve as precursors for the production of different microstructures (e.g. nanocrystalline or partially crystalline alloys) by crystallization under proper heat treatment conditions. In this connection it is important to study the thermal stability, crystallization and the coarsening (grain growth) of the amorphous and nanocrystalline microstructures in order to obtain desirable microstructures for hydrogenation.

Further improvement of the hydriding characteristics of these alloys can be achieved by alloying and by use of small additions of catalyst. Recently, it has been shown, that alloying with Y improves the rate capability and the discharge capacity of Mg_2Ni hydrogen storage alloy type electrodes [8]. Y improves the electrolytic activity, as Y or the YNi_3-phase acts as an active site for hydriding/dehydriding, as well as it increases the lattice parameter of the alloy, which should lead to faster H-diffusion. On the other hand, additions of a third element (like Y) stabilizes the nanostructure of this alloy, which could be very important for practical H-storage materials on the base of Mg_2Ni. In multi-component Mg-based hydrogen storage alloys surface segregation and formation of microcrack passages for H-diffusion improve the kinetics of hydriding [9]. The best kinetic properties so far were found in conventionally prepared $Mg_{0.833}Ni_{0.066}Cu_{0.095}MI_{0.006}$ (MI=La-rich mischmetal), which desorbs 4.75 wt.% H at 330°C under 0.1 MPa in 0.5h or 1.55 wt.% H at 260°C under 0.1 MPa in 1h.

The reasons stated above, determined the aim of the present work: to study the hydriding properties of nanocrystalline $Mg_2(Ni,Y)$ alloy, produced by rapid solidification (melt spinning), in order to compare the H-absorption characteristics of this alloy with the conventionally prepared polycrystalline Mg_2Ni as well as with nanocrystalline Mg_2Ni obtained by ball milling. The thermal stability and phase transformations in the as-quenched nanocrystalline $Mg_2(Ni,Y)$ as well as the influence of hydrogen on the thermal stability and microstructure of this alloy were investigated as well, in order to obtain appropriate microstructures for H-storage.

2. Experimental methods

$Mg_{63}Ni_{30}Y_7$ alloy ingots were prepared by induction melting a mixture of pure Mg metal and a Ni–Y alloy in a vacuum induction furnace under the protection of argon gas with a pressure of 500 mbar. Due to the large difference in the melting temperatures and the high vapour pressure of Mg special care has to be taken to prevent massive Mg evaporation during the melting. From the master alloy ingots, ribbons were produced by a single roller melt-spinning technique (copper quenching disc with a diameter of 250 mm and surface velocity of about 35–40 $m\,s^{-1}$) in a helium atmosphere of 400 mbar.

The nature of the as-cast material as well as the crystalline phases in the annealed and hydrogenated ribbons were characterized by x-ray (using Cu K_α radiation) and electron diffraction. The microstructure was studied by TEM (Philips CM200 operated at 200 kV) and SEM (Hitachi S4500).

The chemical composition of the alloy and of certain phases as well as the surface conditions of the samples before and after hydrogen charging were examined by SEM with an energy dispersive spectrometry (EDAX).

Thermal stability and phase transformations in as-quenched and hydrogenated ribbons were studied by means of DSC (TA-Instruments, DSC910 and 2910).

$Mg_{63}Ni_{30}Y_7$ ribbons were hydrogenated electrolytically under galvanostatic conditions in 0.5 M KOH at a current density of $i=$ 5–6 $A\,m^{-2}$. The hydrogen content was measured by a microbalance (SARTORIUS 4501) with an accuracy of 1 μg.

3. Results and discussion

X-ray diffraction pattern of the as-quenched alloy showed only a broad and diffuse maximum characteristic for the amorphous and nanocrystalline (with grain size of few nanometers only) structures, Fig. 1 (curve *a*). The exact chemical composition of the pre-alloy (master alloy) and of the as-cast ribbons was determined by EDAX analysis to be $Mg_{63}Ni_{30}Y_7$, which is close to the intermetallic compound $Mg_2(Ni,Y)$.

Fig. 2 shows TEM (dark field) micrographs and electron diffraction pattern of the as-quenched $Mg_{63}Ni_{30}Y_7$ alloy, which reveal a nanocrystalline microstructure, homogeneous along the ribbon length and thickness, with an average crystal size of about 2–3 nm. From TEM observations there is some evidence that the as-quenched material consists of nanocrystals embedded into an amorphous phase. An effective grain size of about 1.3 nm was calculated from the full-width at half height of the broad diffraction peak in Fig. 1(a), using Scherrer's equation. This value is lower than that determined from TEM and suggests also the presence of an amorphous phase. In the electron diffraction pattern of the as-quenched ribbons only the hexagonal $Mg_2(Ni,Y)$ phase could be detected, i.e. obviously the as-cast material contains $Mg_2(Ni,Y)$ nanocrystals.

The thermal stability and phase transformations in the as-cast alloy were studied by DSC under isothermal and isochronal conditions. Fig. 3 shows the DSC trace of the as-quenched alloy at 5 $K\,min^{-1}$ heating rate. A single exothermic peak was observed at $T_{max}=183$°C (at 5 $K\,min^{-1}$) and with an enthalpy change ΔH_x of 100 ± 3 $J\,g^{-1}$. Most probably this peak is associated with crystallization of the amorphous phase, existing between the nanocrystals. For comparison, crystallization of $Mg_{65}Cu_{25}Y_{10}$ amorphous alloy was found to proceed at

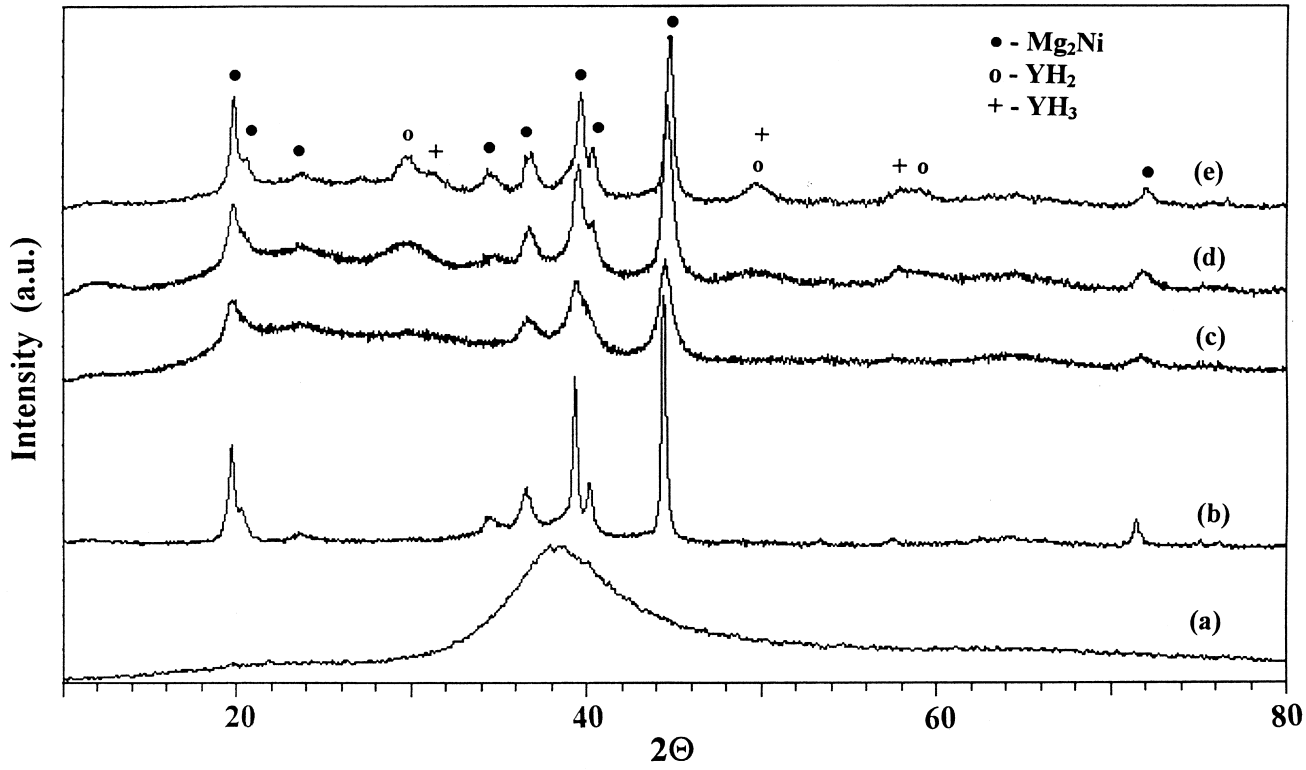

Fig. 1. X-ray diffraction patterns (Cu K_α) of (a) as-quenched, (b) crystallized at 300°C, (c) hydrogenated and then crystallized at 220°C, (d) hydrogenated and crystallized at 310°C and (e) hydrogenated and crystallized at 400°C $Mg_{63}Ni_{30}Y_7$ alloys.

about 215°C (at 40 K min^{-1} heating rate) [10]. Crystallization of $Mg_{55}Cu_{30}Y_{15}$ and $Mg_{50}Ni_{30}Y_{20}$ glasses was observed at 230°C [11] and 265°C [10], respectively. The Mg_2Ni type phase in $Mg_{50}Ni_{50}$ amorphous alloy crystallizes at 320°C [12]. The thermal effect (crystallization peak) observed (Fig. 3) shows a sharp beginning and a small tail, which implies that a second crystallization reaction proceeds (to a much smaller degree than the first reaction). From the relatively large enthalpy difference (ΔH_x) of overall crystallization (about 100 J g^{-1}) can be concluded that the as-quenched material contains a significant amount of amorphous (disordered) phase. The activation energy of this transformation was estimated according to the Kissinger method [13] to be 140±7 kJ mol^{-1}, Fig. 4. This value coincides exactly with the activation energy of Mg self-diffusion, 138±2 kJ mol^{-1} [14]. Activation energies in the range of 160–240 kJ mol^{-1} for crystallization of Mg_2Ni type phase in amorphous Mg(Ni,TM), depending on the concentration of the 3d transition metal (TM), have been also recently reported [12].

In order to clarify the mechanism of the transformation observed, an isothermal DSC study was carried out (at 188°C). The Avrami exponent, $n=3$, obtained can be interpreted in terms of the JMA formalism as three-dimensional growth of a constant number of nanocrystals, already existing in the as-quenched material, occurring during the heat treatment. This result is in agreement with our TEM investigation. In this way the activation energy of 140 kJ mol^{-1} has to be attributed to the process of nanocrystals growth. This relatively low activation energy (for crystallization of a metallic glass) is in accordance with the proposed transformation mechanism that only growth of existing nanocrystals has occurred during the annealing of the as-quenched $Mg_{63}Ni_{30}Y_7$ alloy. Obviously formation of new crystalline nuclei (nucleation) does not proceed during annealing.

The X-ray diffraction pattern of the completely crystallized $Mg_2(Ni,Y)$ alloy is shown in Fig. 1 (curve *b*). It reveals that the main crystalline phase is similar to that of the hexagonal Mg_2Ni (a_o=5.21 Å, c_o=13.23 Å). The lattice constants are slightly increased (a_o=5.28 Å, c_o= 13.48 Å) as expected when Ni is partially substituted for Y in the Mg_2Ni lattice, because of the larger atomic radius of Y than Ni. Besides the $Mg_2(Ni,Y)$ phase, only traces of $Mg(Ni,Y)_2$ can be detected, obviously connected with the small exothermic effect at the end of the crystallization peak. TEM also shows that the crystallized alloy (annealed at 300°C for short time) consists mainly of the hexagonal $Mg_2(Ni,Y)$ phase, as the crystals in the fully crystallized ribbon have grain sizes of about 80–90 nm, Fig. 5. SEM study from the cross-section of the ribbon also confirms that the completely crystallized alloy consists of crystals with grain sizes less than 100 nm.

In order to study the hydriding properties of the nanocrystalline $Mg_{63}Ni_{30}Y_7$ (maximum H-absorption capacity, kinetics of hydriding/dehydriding) as well as the

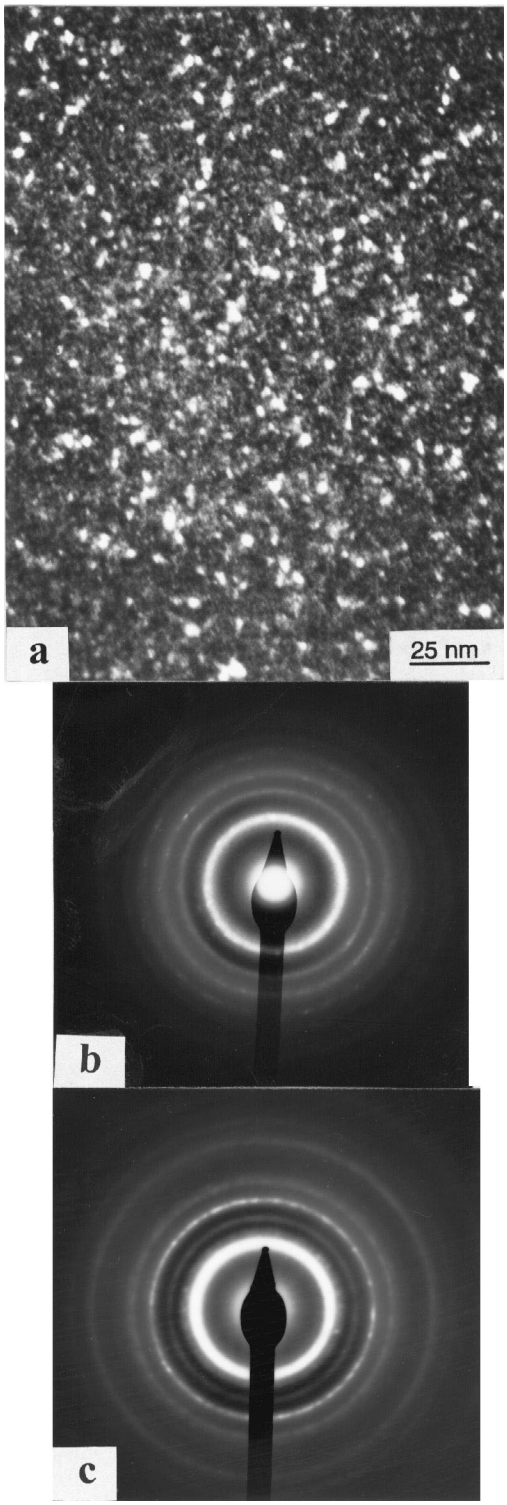

Fig. 2. TEM image (dark field) and electron diffraction pattern of as-quenched (a,b) and electron diffraction pattern of H-charged nanocrystalline $Mg_{63}Ni_{30}Y_7$ (c).

influence of hydrogen on the thermal stability and microstructure before and after annealing, the as-quenched alloy was electrolytically hydrogenated. Surface oxidation after hydrogen charging was not observed. Slight oxidation was

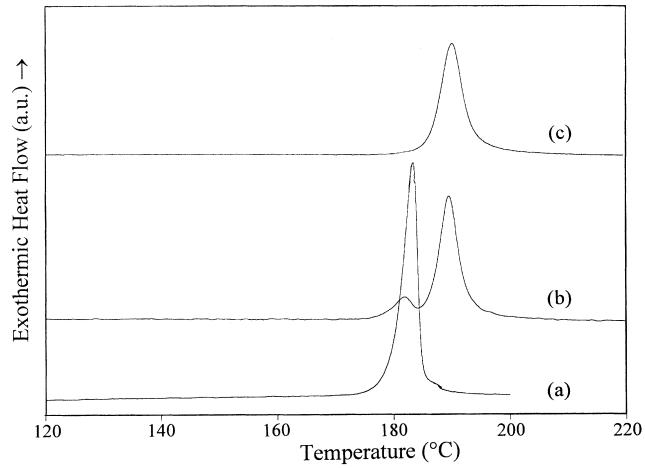

Fig. 3. DSC curves (at 5 K min^{-1} heating rate) of (a) as-cast, (b) hydrided (about 2 wt.% H) and (c) hydrided (about 3 wt.% H) $Mg_{63}Ni_{30}Y_7$ alloys.

detected only after long time of hydrogenation ($t \geq 4$ h). Fig. 6 shows the rate of hydrogen absorption by the as-cast alloy. The amount of the hydrogen absorbed increases with the time of hydrogenation showing a saturation at times longer than 1 h; finally it reaches 3.0 wt.% ($Mg_2(Ni,Y)H_{3.5}$). The results on the kinetics of hydrogen absorption from the gas phase (at 200°C and pressure 15 bar) of nanocrystalline ball-milled Mg_2Ni alloys obtained by Zaluski et al. [4], plotted in Fig. 6 too, show a good agreement with our kinetic curve. Similar to our previous results on hydrogenation of $Mg_{82}Ni_{11}Y_7$ and $Mg_{54}Cu_{36}Y_{10}$ alloys [15], the hydrogenation of the present alloy (Fig. 6) exhibits a very fast hydrogen absorption stage in the beginning (during the first 30–40 min of hydrogenation), after which the hydrogen content is saturated with the time of hydrogenation longer than 1 h, without reaching the maximum value reported for this alloy, 3.6 wt.% H (corresponding to Mg_2NiH_4). Also Zaluski et al. [4] found that at low temperatures the total amount of hydrogen absorbed in nanocrystalline Mg_2Ni

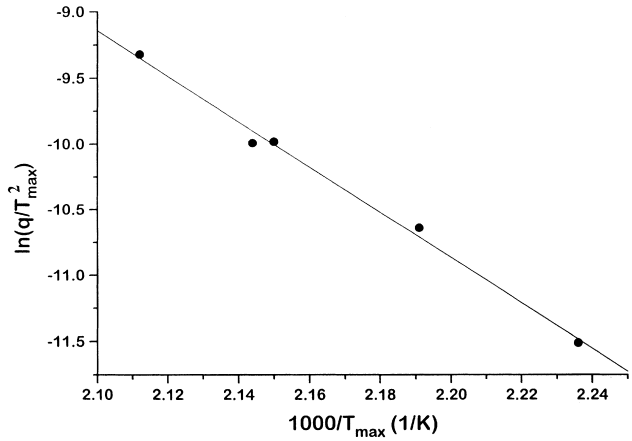

Fig. 4. Kissinger plot of the maximum temperature for the DSC exothermic (crystallization) peak for hydrogen free $Mg_{63}Ni_{30}Y_7$ alloy.

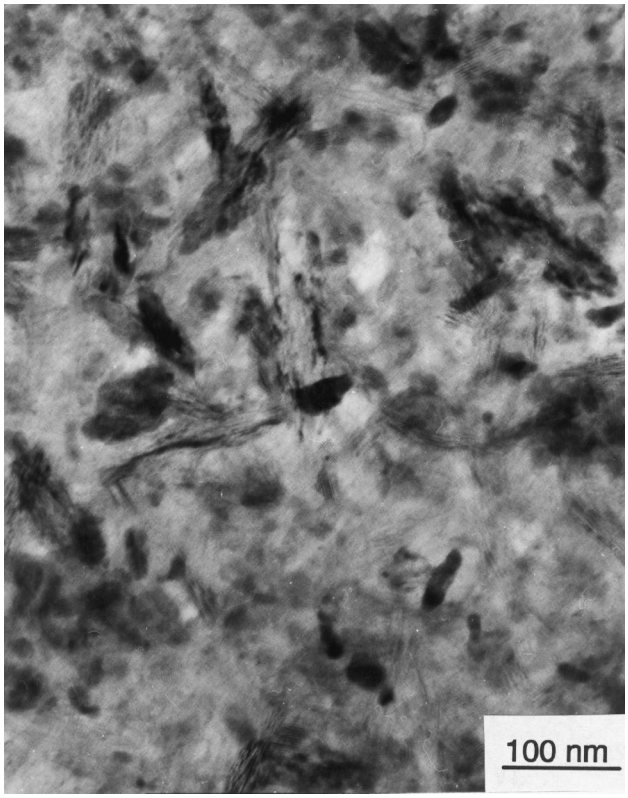

Fig. 5. TEM micrograph of the microstructure of crystallized (at 300°C) $Mg_{63}Ni_{30}Y_7$.

(H-charged from gas phase) for 1h is relatively low (about 2–3 atoms H per formula Mg_2Ni).

Orimo et al. [6] reported about a maximum hydrogen capacity of 1.6 wt.% ($Mg_2NiH_{1.8}$) of a nanostructured composite material of the Mg_2Ni-H system synthesised by reactive mechanical grinding under a hydrogen atmosphere. The authors found no traces of the hydride phase Mg_2NiH_4 even after grinding for 80 h. They observed a rapid increase of the hydrogen content after the first 15 min grinding, which is explained with hydrogen occupation in the disordered (amorphous) interface phase around the nanocrystalline Mg_2Ni. Transformation of the amorphous phase into crystalline Mg_2NiH_4 was supposed to take place during annealing at 473 K, before the complete hydrogen desorption [6]. It is necessary to be mentioned that the melt-spun nanocrystalline $Mg_{67}Ni_{30}Y_7$ alloy in the present study contains substantially larger amount of amorphous phase compared with the mechanically ground Mg_2Ni studied by Orimo et al. [6], which might be the reason for the higher hydrogen content determined by us. Although direct comparison between the maximum hydrogen content (hydrogen capacity) of the melt-spun nanocrystalline alloy in the present work and the nanostructured mechanically ground Mg_2Ni [6] is not correct, because of different hydrogen charging conditions, the results from both studies support the suggestion that the hydriding properties of nanocrystalline materials are mainly affected by the disordered regions at the interfaces of the nanocrystals. It is expected that in the case of nanocrystalline alloys containing large amount of amorphous phase between the nanocrystals the solid state H-solubility is further increased as compared to the nanocrystalline alloys without amorphous phase [4]. As in our previous study [15] we assume that hydrogenation of the present alloy begins with a fast diffusion of interstitial hydrogen in the grain boundary regions (with filling by H of the easily accessible sites at the disordered (amorphous) grain boundaries [16]), which act as easy pathways for the hydrogen diffusion.

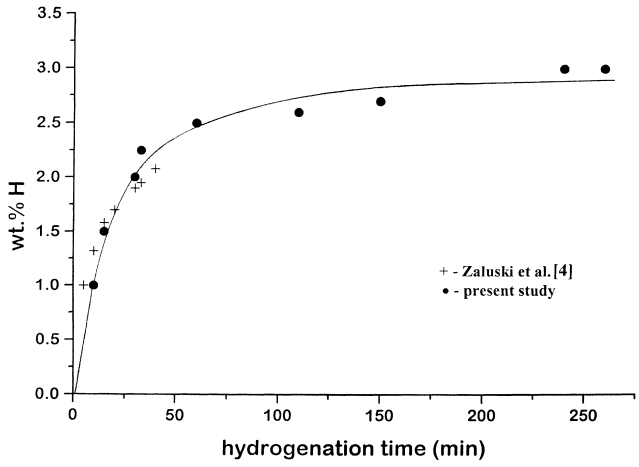

Fig. 6. Rate of hydrogen absorption for as-cast $Mg_{63}Ni_{30}Y_7$ (+ - results of Zaluski et al. [4] for ball-milled Mg_2Ni, hydrogenated from a gas phase at 200°C and pressure 15 bar).

After hydrogen charging of the as-cast alloy, the X-ray diffraction pattern contains only broad and diffuse maximums, similar to the as-quenched H-free sample. TEM observations and electron diffraction (Fig. 2 (c)) of hydrogenated as-quenched alloys also revealed a nanocrystalline microstructure, as $Mg_2(Ni,Y)$ nanocrystals were only detected. The average grain size, as determined by TEM, remains about 2–3 nm after hydrogen charging.

The crystallization of hydrogenated $Mg_{67}Ni_{30}Y_7$ alloy has been studied as well. DSC measurements at relatively low hydrogen concentration (less than 1 wt.% H) show no significant changes in the temperature and enthalpy of crystallization (actually growth of nanocrystals in the amorphous matrix) compared with the hydrogen free as-cast alloy. Increasing the hydrogen concentration of the alloy, however, leads to splitting of the exothermic DSC peak in two clearly distinguished exothermic peaks and finally (at hydrogen concentrations higher than about 2.5 wt.%) to a single exothermic peak, shifted by 7 K to higher temperatures compared with the crystallization peak of the hydrogen-free alloys (T_{max}=190 at 5 K min^{-1}), Fig. 3. Due to hydriding of the as-quenched alloy the crystallization enthalpy, ΔH_x, reduces from 100 J g^{-1} for the unhydrided to 80 J g^{-1} for the H-charged alloys, indicating also a change in the crystallization reaction after hydriding,

probably connected with the nanocrystalline product of the crystallization.

X-ray diffraction patterns of alloys hydrogenated and then heat treated at different temperatures above the crystallization reaction alloys are shown in Fig. 1 (curves *c–e*). The main diffraction peaks correspond to the hexagonal Mg_2Ni phase, as the lattice constants are slightly increased, because of the hydrogen dissolved into the Mg_2Ni phase, i.e. the hydrogen solid solution Mg_2NiH_x phase ($x \approx 0.3$, estimated from the crystal lattice expansion) is formed during heating. The hydride phase Mg_2NiH_4 was not detected, even after long time of hydrogenation. The diffraction peaks of the hydrogenized and then crystallized samples, however, are shifted to higher angles as compared with those of the crystallized H-free alloy. This effect can be explained by the crystallization of $Mg_2NiH_{0.3}$, instead of $Mg_2(Ni,Y)$, because of yttrium hydrides formation during hydriding and subsequent annealing. Indeed, broad diffraction peaks of YH_2 and YH_3 are clearly seen for hydrogenated and then crystallized samples, Fig. 1 (curves *c–e*). TEM and electron diffraction of hydrogenized (with more than 2 wt.% H) and then crystallized alloys show that the sample is composed of Mg_2NiH_x ($x \approx 0.3$) crystals without sharp boundaries. The average crystals size is estimated to be 15 nm for the samples annealed at 220°C, Fig. 7. Annealing at 310°C does not lead to substantial increasing of the nanocrystals size, which remains in the range 15–20 nm, Fig. 7. The electron diffraction also reveals the nanocrystalline nature of the hydrogenated alloy after annealing at 310°C, Fig. 7. The X-ray diffraction patterns of hydrogen charged and then crystallized alloys, Fig. 1 (curves *c,d*) exhibit broadening of the peaks

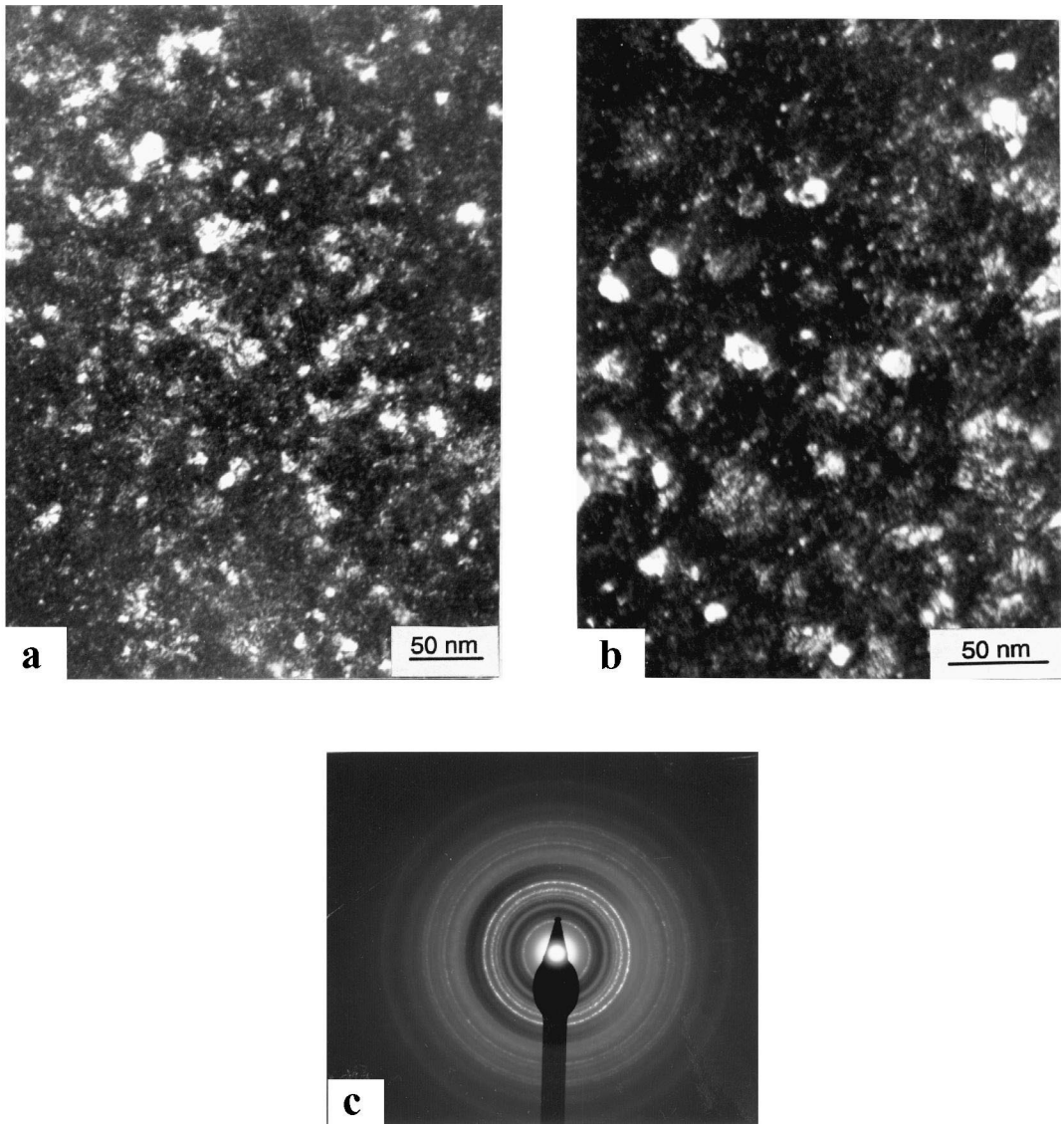

Fig. 7. TEM image of hydrided and then crystallized at 220°C (a) and TEM image and electron diffraction of hydrided and crystallized at 310°C $Mg_{63}Ni_{30}Y_7$ (b,c).

characteristic for nanocrystalline material and also confirm the results from TEM and electron diffraction.

The small size of the crystals (about 15–20 nm) of the main $Mg_2NiH_{0.3}$ phase indicates that the volume fraction of the disordered grain boundary phase is still large, although it is much smaller then the volume fraction of the disordered (amorphous) phase in the as-quenched nanocrystallne (with 2–3 nm grain size) material. According to an estimation of Orimo et al. [6] the volume fraction of the disordered inter-grain region in nanocrystalline Mg_2Ni with grain size of 15 nm is about 30% of the total volume. Due to this big volume fraction of disordered inter-grain phase in the crystallized hydrided alloy the total amount of the absorbed hydrogen remains also large after crystallization. We would like to mention once again that crystallization of the hydride phase Mg_2NiH_4 was not detected during the heat treatment of the hydrogenated alloy, although the hydrogen concentration in the disordered grain boundary phase is close to that in the Mg_2NiH_4 phase.

Careful examination of the position of the diffraction peaks of the hexagonal Mg_2NiH_x (Fig. 1, curves *c–e*) reveals a continuous decrease of the lattice constants with increasing the temperature of annealing, approaching the values for the pure Mg_2Ni, which indicates hydrogen desorption during annealing. Desorption of hydrogen has been also detected by DSC (under scanning conditions) as a broad endothermic effect starting at about 250°C. Similar temperatures for hydrogen desorption from Mg_2Ni alloys (250–300°C) were also reported by Orimo et al. [6], Song [17] and Akiyama et al. [2]. Unfortunately the total enthalpy of H-desorption, ΔH_{des}, could not be determined from the DSC scan, because of the exothermic oxidation reaction (although the experiments were carried out under pure nitrogen) starting at about 300– 350°C. Annealing at 400°C after hydrogenation, however, leads to a noticeable increase in the crystals size. Grain growth is observed at temperatures at which a substantial amount of hydrogen is already desorbed. At these annealing temperatures (about 400°C), except the main Mg_2Ni phase, YH_2 and YH_3 are only present, Fig. 1 (e), because of the higher stability of these hydrides in comparison to Mg_2NiH_x and MgH_2. Rare-earth hydrides (incl. yttrium hydrides) formed during the first hydriding process are supposed to serve as catalysts for the hydriding reaction and practically do not participate in the further absorption-desorption cycles [18].

The influence of hydrogen on the crystallization, observed in rapidly quenched $Mg_2(Ni,Y)$ alloys, can be summarised in the following way: During charging the as-cast alloy hydrogen dissolves mainly in the amorphous phase around the $Mg_2(Ni,Y)$ nanocrystals, reaching total concentration of 3.0 wt.% ($Mg_2(Ni,Y)H_{3.5}$). Subsequent heat treatment of the hydrided alloy leads to crystallization of the amorphous phase mainly into the hydrogen solid solution Mg_2NiH_x ($x \approx 0.3$) phase and yttrium hydrides. The formation of the Mg_2NiH_4 phase was not detected. The microstructure of completely crystallized H-charged alloys remains nanocrystalline (15–20 nm). After dehydriding (at temperatures below 400°C) the alloy consists of Mg_2Ni and nanocrystalline yttrium hydrides (YH_2 and YH_3).

Finally, on the basis of the results presented above we can conclude that rapidly quenched nanocrystalline Mg_2Ni-based alloys show hydriding properties (hydrogen capacity and hydrogenation kinetics) comparable to those of the ball-milled nanocrystalline materials and superior to the polycrystalline Mg_2Ni alloys. On the other hand, this study shows that nanocrystalline Mg_2Ni-based alloys, containing a large amount of the amorphous phase can serve as successful precursor for producing stable nanocrystalline microstructures for hydrogen storage.

4. Conclusion

Thermal stability and phase transformation in nanocrystalline $Mg_{63}Ni_{30}Y_7$, produced by melt spinning, were studied by TEM, DSC, x-ray and electron diffraction. The as-quenched alloy was found to consist of mainly hexagonal $Mg_2(Ni,Y)$ nanocrystals, with an average size of about 2–3 nm embedded in an amorphous phase. During heating the alloy crystallizes completely (the reaction starts at about 180°C at 5K min^{-1} heating rate) by three dimensional growth of the quenched-in nanocrystals with an activation energy of 140 ± 7 kJ mol^{-1}.

The hydriding properties of the as-quenched nanocrystalline $Mg_{63}Ni_{30}Y_7$ alloy were studied as well. It was found that the maximum H-absorption capacity of the melt-spun alloy (about 3.0 wt.% H) is comparable with that of the nanocrystalline Mg_2Ni, produced by ball-milling. The hydrogenation kinetics of the melt spun alloy (charged electroltically at room temperature) showed also similarities with the nanocrystalline ball milled Mg_2Ni (hydrogenated from gas phase at 200°C under 15 bar). The initial very fast hydrogen absorption is assumed to be due to rapid diffusion of hydrogen in the grain boundary regions (disordered, amorphous phase between the nanocrystals). Hydrogenation of the as-quenched nanocrystalline $Mg_{63}Ni_{30}Y_7$ leads to a change in the phase transformation (crystallization of the amorphous phase) during annealing of the alloy, as the microstructure remains nanocrystalline even after heating up to 300–350°C, i.e. after the complete crystallization of the alloy.

Although the as-quenched nanocrystalline $Mg_2(Ni,Y)$ alloys, containing large amounts of amorphous phase, are not stable for repeating hydrogenation and dehydrogenation (because of relatively high temperature of H-desorption) the present study shows that by careful control of the quenching and/or heat treatment conditions stable nanocrystalline microstructures for hydrogen storage can be attained.

Acknowledgements

One of the authors (T. Spassov) is very grateful to the Alexander von Humboldt Foundation (Germany) for financial support.

References

[1] R.L. Holtz, M.A. Imam, J. Mat. Sci. 32 (1997) 2267.
[2] T. Akiyama, T. Fukutani, R. Takahashi, J. Yagi, Mater. Trans. 37 (1996) 1014.
[3] R.L. Holtz, V. Provenzano, M.A. Imam, NanoStr. Mater. 7 (1996) 259.
[4] L. Zaluski, A. Zaluska, J.O. Ström-Olsen, J. Alloys Comp. 253–254 (1997) 70.
[5] L. Zaluski, A. Zaluska, J.O. Ström-Olsen, J. Alloys Comp. 217 (1995) 245.
[6] S. Orimo, H. Fujii, K. Ikeda, Acta mater. 45 (1997) 331–341.
[7] S. Orimo, H. Fujii, J. Alloys Comp. 232 (1996) L16.
[8] N. Cui, B. Luan, H.J. Zhao, H.K. Liu, S.X. Dou, J. Alloys Comp. 233 (1996) 236.
[9] M. Au, J. Wu, Q. Wang, Int. J. Hydrogen Energy 20 (1995) 141.
[10] A. Inoue, T. Masumoto, Mat. Sci. Eng. A173 (1993) 1.
[11] N. Schlorke, J. Eckert, L. Schultz, Mat. Sci. Forum. 269–272 (1998) 761.
[12] S. Orimo, K. Ikeda, H. Fujii, K. Yamamoto, J. Alloys Comp. 260 (1997) 143.
[13] H. Kissinger, Anal. Chem. 29 (1957) 1702.
[14] Landolt-Börnstein, III/26, Springer Verlag Berlin, 1990, p. 38.
[15] U. Köster, D. Zander, H. Alves, T. Spassov, in: Proceedings of the First Israeli International Conference on Magnesium Science and Technology, Dead Sea, 1997, in press.
[16] U. Stuhr, H. Wipf, T.J. Udovic, J. Weissmüller, H. Gleiter, J. Phys.: Condens. Mater. 7 (1995) 219.
[17] M. Song, J. Mat. Sci. 30 (1995) 1343.
[18] B. Darriet, M. Pezat, A. Hbika, P. Hagenmuller, Int. J. Hydrogen Energy 5 (1980) 173.